

## Influence of Oleic Acid (Vegetable Oils) and TiO<sub>2</sub> Addition on the Optical Properties and Chromaticity of Chitosan Composite Films

<sup>1</sup>Elham M. Hussien, <sup>1</sup>W. M. Desoky, <sup>1</sup>Magda S. Hanafy and <sup>2</sup>Osiris W. Guirguis

<sup>1</sup>Department of Physics, Faculty of Science, Zagazig University, Zagazig, Egypt

<sup>2</sup>Department of Biophysics, Faculty of Science, Cairo University, Giza, Egypt

**Key words:** Chitosan, TiO<sub>2</sub> nanoparticles, Oleic acid, Optical properties and chromaticity

**Abstract:** Cs/OA/TiO<sub>2</sub> (NPs) composite films were synthesis via conventional solution casting technique. The chromaticity, CIE tristimulus values, color parameters and optical properties of Chitosan, Cs, films with the addition of TiO<sub>2</sub> and Oleic acid were investigated using the transmittance and reflectance measurements of the spectrophotometric. The absorption,  $\alpha$ , coefficient of the composite films were estimated. Therefore, the optical band gaps and their type were estimated with effect of additions. The refractive index of the films was estimated. Subsequently, the lattice dielectric constant  $\epsilon_L$  and the ratio of the number carriers concentration to their effective mass, the real ( $\epsilon_1$ ) and imaginary ( $\epsilon_2$ ) parts of the dielectric constants, complex optical conductivity (real,  $\sigma_1$  and imaginary,  $\sigma_2$ ), The volume energy loss function, VELF and the surface energy loss function were calculated. Moreover, Opto-electrical parameters such as the relaxation time, optical mobility and optical resistivity were extracted using the Drude theory. The developed Chitosan films supporting an optimized amount of TiO<sub>2</sub> (NPs) and Oleic acid could be employed in industry and medicine applications.

### Corresponding Author:

Elham M. Hussien

Department of Physics, Faculty of Science, Zagazig University, Zagazig, Egypt

Page No.: 3660-3667

Volume: 15, Issue 22, 2020

ISSN: 1816-949x

Journal of Engineering and Applied Sciences

Copy Right: Medwell Publications

## INTRODUCTION

The biopolymers composite films with a different kind of nanoparticle filler attract enormous attention due to their structure, electric, thermal, optical, abundant, low cost, renewable and their potential applications in industry and medicine<sup>[1-3]</sup>. The renewable biopolymers such as lipids, polysaccharides, proteins and their composites, derived from plant and animal resources<sup>[1]</sup>. Biopolymer-based edible films and coatings are utilized to improve the quality of food preservation by isolating against oxygen, moisture, flavor and odor. Moreover, polymer films are

brilliant mediums for incorporating a wide assortment of additives such as antifungal, antioxidants, antimicrobial agents, colors and other nutrients<sup>[2]</sup>.

Vegetable or plant oils demonstrate a renewable resource that can be utilized as starting material to access novel products with a broad array of structural and utilitarian varieties. The low cost and the abundant availability of plant oil make an industrially attention for many applications such as plastics industry. Naturally occurring plant oils and fatty acids derived there of are considered to be the most important renewable feedstock processed in the preparation of bio based functional

polymers and polymeric materials<sup>[3-6]</sup>. The main constituents of plant oils are triglycerides which are the product of esterification of glycerol with three fatty acids. Fatty acids account for 95% of the total weight of triglycerides and their content is characteristic for each plant oil. Chitosan is recognized as one of the effective polymers among several commercially available biopolymers due to their application as antimicrobial and antioxidants to improve quality of food<sup>[2, 7]</sup>. The addition of oleic acid to biopolymer promotes significant changes in the size and surface charges of the film also decreases the hydrophilicity. The major disadvantages of blending or reinforcing natural polymers with artificial polymer are their incompatibility with the matrix, which is produced by the immiscibility of the hydrophilic natural polymers with the hydrophobic artificial polymers<sup>[2, 8]</sup>. Titanium dioxide, TiO<sub>2</sub> is utilized as a safe nanostructured material for polymeric applications, enhancing toughness and barrier properties as well as providing brightness and antibacterial effects<sup>[9]</sup>. Oleic acid may be bound to the TiO<sub>2</sub> surface by chelating and bridging bidentate; this may increase compatibility between TiO<sub>2</sub> and hydrophobic solutions and to possibly obtain stable dispersions of TiO<sub>2</sub> in the Chitosan matrix<sup>[10]</sup>. The aim of this study is to develop the kind of multifunctional composite material to meet the need of high adsorption, nontoxic, environmental-friendly and cost effective with enhanced optical and antibacterial properties. For this purpose, the nanocomposite films of Chitosan with different additions of TiO<sub>2</sub> (NPs) and Oleic Acid (OA). The (Cs, Cs/TiO<sub>2</sub>, Cs/OA and Cs/OA/TiO<sub>2</sub>) composite films were synthesized using casting solution method. The crystal structural, morphological and thermal properties of such films were performed using X-Ray Diffraction (XRD), High-Resolution Transmission Electron Microscopy (HRTEM), field emission scanning electron microscopy (FESEM), Fourier Transform Infrared spectroscopy (FTIR) and Thermal Analysis (TGA and DSC) were studied in early reference for the same researchers<sup>[3]</sup>. Subsequently, this allows us to study the optical CIE tristimulus values, color parameters, chromaticity properties, absorption index and refractive index and correlated with their structure of the prepared films. The obtained results are crucial data to improve the properties of these films for many applications, especially for antibacterial applications.

## MATERIALS AND METHODS

**Experimental:** The pure Chitosan (Cs), the Chitosan/titanium dioxide nanoparticles (Cs/TiO<sub>2</sub>(NPs)), the Chitosan/Oleic acid (Cs/OA) and the Chitosan /TiO<sub>2</sub> NPs/Oleic acid (Cs/OA/TiO<sub>2</sub>), bio-composite films were synthesized using solution casting technique<sup>[2, 11]</sup>. The samples named Cs, Cs/OA, Cs/TiO<sub>2</sub> and Cs/OA/TiO<sub>2</sub>,

respectively. The pure Chitosan films were prepared by adding 0.5 g Chitosan dissolved in 100 mL of (1% w/v) of an aqueous solution of 0.1 M glacial acetic acid at room temperature. The solution was stirred for 24 h using a magnetic stirrer left overnight with continuous stirring until becoming homogenous. The unsolvable clumps in the solution were removed using filtration. The films (about 0.2 mm in thickness) were constructed using the decanting method of clear mixture into Petri dishes with radius 6 cm. The solution in the Petri-dishes left around 4 days. Once dried, the films were peeled off softly from the plates. To prepare Cs/TiO<sub>2</sub> (NPs) composite films, the TiO<sub>2</sub> NPs were added to Cs solution, separately. The Digital Ultrasonic model CD-4820 170 W/42 kHz was utilized for 1 h to avoid TiO<sub>2</sub> agglomeration and obtain good diffusion in the solutions. The TiO<sub>2</sub> converted into Titanium cations (Ti<sup>+4</sup>) when the Cs and TiO<sub>2</sub> (NPs) were dissolved in dilute CH<sub>3</sub>COOH, then coordination links -OH and -NH<sub>2</sub> groups of Cs chains immediately created Ti<sup>+4</sup> ions. The solution poured into Petri dishes and left for 24 h at 40°C to dry. The (Cs/OA) film prepared by added 1 mL of oleic acid to Chitosan solution and stirred using a magnetic stirrer for 24 h at 25°C. Then the solution poured into Petri dishes and dried at 40°C for 24 h. The dried films were gently removed served. The (Cs/OA/TiO<sub>2</sub>) composite films prepared by adding 1 mL of oleic acid and 15 wt% of TiO<sub>2</sub> nano-powders to the Cs solutions and stirred for 24 h at 25°C. The mixture solutions dried at 40°C for 24 h. These films were peeled off and served<sup>[3]</sup>. A UV/VIS/NIR Double Beam Spectrophotometer (Shimadzu) with standard illuminate (C) has been used to measure the reflectance, R(λ) and the transmittance, T(λ) for the prepared composite films in the wavelength range 190-1800 nm at room temperature. From the obtained spectra, the optical CIE tristimulus values, color parameters, chromaticity properties, absorption index and refractive index have been calculated. The experimental errors are studied as follows ±0.2% for T and R measurements. While the error of refractive index, absorption index and the film thickness are ±3, ±2.5 and 4%, respectively.

## RESULTS AND DISCUSSION

**Optical properties:** Transmittance, T(λ) and reflectance, R(λ) for Cs, Cs/TiO<sub>2</sub>, Cs/OA and Cs/OA/TiO<sub>2</sub> nanocomposites films were measured as shown in Fig. 1. There is an observable decrease in the reflectance and increase in transmittance values for the whole spectrum. While the R and T decrease with added oleic acid and TiO<sub>2</sub> at constant frequency. This decrease may be attributed to decreases the transparency of the films which may be due to the variation in the molecular configuration. Figure 2 illustrates the calculated tristimulus reflectance values, X<sub>r</sub>, Y<sub>r</sub> and Z<sub>r</sub>,

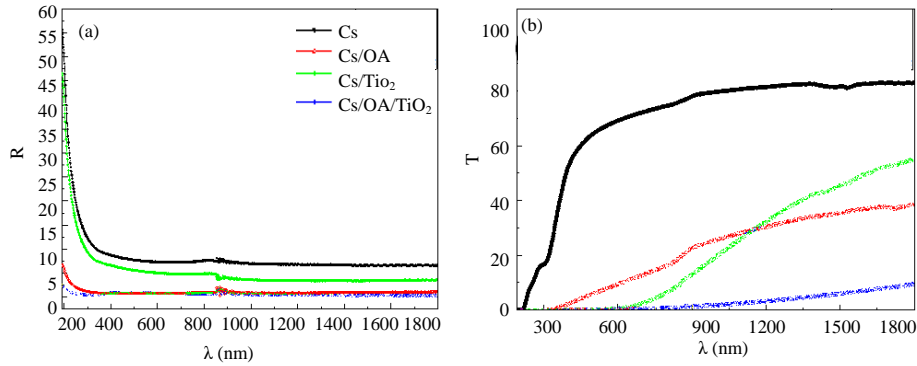


Fig. 1(a, b): The spectral distribution of (a) reflectance and (b) transmittance Cs, Cs/TiO<sub>2</sub>, Cs/OA and Cs/OA/TiO<sub>2</sub> composite films

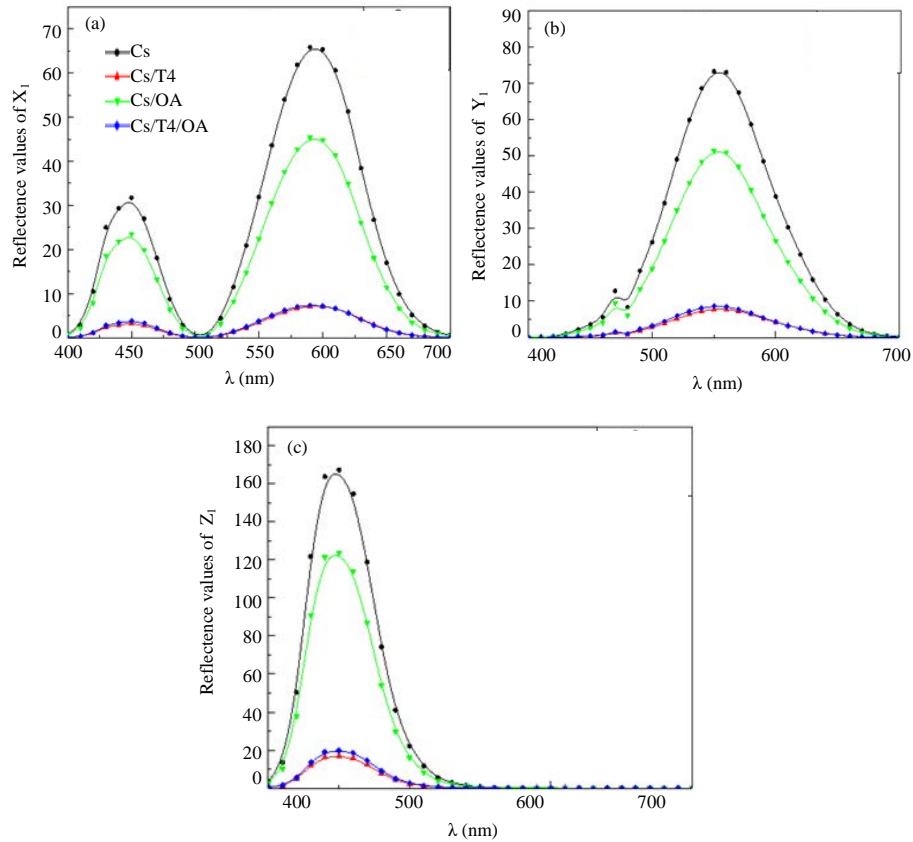


Fig. 2 (a-c): The variation of the tristimulus reflectance values of (a)  $X_r$ , (b)  $Y_r$  and (c)  $Z_r$  as functions of wavelength for Cs, Cs/TiO<sub>2</sub>, Cs/OA and Cs/OA/TiO<sub>2</sub> composite films

forsynthesized composite films as a function of wavelength follow the procedure in reference<sup>[11, 12]</sup>. It is clear that, the peaks position are nearly the same for each tristimulus values with different concentrations, while the peaks intensity decrease with the addition of TiO<sub>2</sub> and OA. Subsequently, the color constants ( $a^*$  and  $b^*$ ), relative brightness values ( $L^*$ ), whiteness index ( $W$ ),

chroma ( $\Delta C^*$ ), hue ( $\Delta H^*$ ), yellowness ( $Y_e$ ) and the color difference ( $\Delta E^*$ ) were also calculated following the early references<sup>[12, 13]</sup>.

From Table 1, the relative brightness ( $L^*$ ) values in the composite films with oleic acid lead to decrease in its value with adding oleic acid. The value color constants ( $a^*$  and  $b^*$ ) increase with adding oleic acid which

Table 1: The obtained results of color parameters and their percentage changes for Cs, Cs/TiO<sub>2</sub>, Cs/OA and Cs/OA/TiO<sub>2</sub> composite films

	Cs	Cs/TiO <sub>2</sub>	Cs/OA	Cs/OA/TiO <sub>2</sub>
L*ΔL%	5.5397	5.4845	5.6086	5.5531
a*	-0.0099	-0.0304	-0.0271	-0.2975
Δa*%		205.6	-127.1	-2.886.5
b*	-0.3222	-0.5398	-0.0674	-0.3668
Δb*%		67.6	79.1	-13.8
W	-2.3531	-2.2372	-2.4949	-2.2498
ΔW%	-	-4.9	-6.0	4.4
Ye	-10.5140	-17.9742	-2.4906	-15.622
Δye%	-	71.0	76.3	-48.5
ΔE*	-	0.23	0.26	0.29
ΔC*	-	0.11	0.24	0.15
ΔH*	-	0.19	0.07	0.24

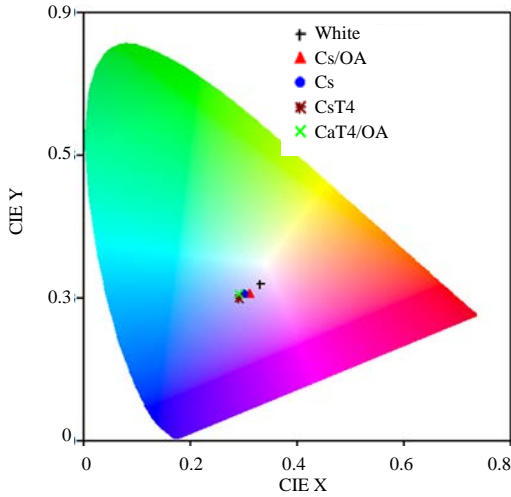


Fig. 3: Chromaticity diagram with superimposed the chromaticity points of Cs, Cs/TiO<sub>2</sub>, Cs/OA and Cs/OA/TiO<sub>2</sub> composite films

indicates that there is an increase in green component instead of red one and increase in yellow component instead of blue one receptivity. In other hand, the whiteness index (W) decreases with adding oleic acid. In total, the change in color scales such as E\*, C\* and H\* indicate that there are small variations in color between the composite films which occurred due to adding oleic acid in the composites. The chromaticity coordinates can be calculated using the obtained tristimulus values as fractions of their total as follow<sup>[14]</sup>:

$$X = \frac{x}{X+Y+Z}, Y = \frac{Y}{X+Y+Z}, Z = \frac{Z}{X+Y+Z} \quad (1)$$

where x, y and z are the chromaticity parameters of red, green and blue light in the samples, respectively. The chromaticity would require a three-dimensional coordinate system which is not practicable. The coordinates z is dependent on x and y where (x+y+z = 1), so only x and y are acceptable to describe of the sample color in the two-dimensional diagram. The reference

point, white, theoretically corresponds to x, y or z, each having values of 0.333. While the number 0 and 1 indicate to color absent and pure red, green or blue, respectively<sup>[14]</sup>.

Figure 3 illustrates the change of chromaticity values for composite films with oleic acid in comparison with the white point in two dimensions. The results suggest that all samples have nearly the same color with small shift to blue color from the white point. The shift may be due to the change in the physical bonds and then changes in the molecular configuration of composite films. In order to investigate the optical energy gap, E<sub>g</sub>, the absorption coefficient, α as a function of photon energy of the composite films have been calculated using the following relation<sup>[15,16]</sup>:

$$\alpha = \frac{1}{d} \ln \left[ \frac{(1-R)^2}{2T} + \sqrt{\frac{(1-R)^4}{4T^2} + R^2} \right] \quad (2)$$

$$\alpha h\nu = B(h\nu - E_g)^m \quad (3)$$

Also, inset figure shows the absorption coefficient, α, of Cs, Cs/TiO<sub>2</sub>, Cs/OA and Cs/OA/TiO<sub>2</sub> composite films.

Figure 4, inset figure, illustrates the absorption coefficient against photon energy, hν and the relation between against of studied composite films. Using (Eq. 3) with (Fig. 4), the value of 2 which it indicates that the most predominate mechanism is allowed direct transition and the values of optical energy gaps, E<sub>g</sub> were extracted for each sample from the points of intercept with the x-axis. The extracted E<sub>g</sub> were found 2.64, 1.7, 2.22, 2.00 eV, respectively. These gaps can be referred to the energy separation between the minimum conduction band and the maximum valence band of studied composite films. The values of optical energy gaps decrease with added OA and TiO<sub>2</sub>. The refractive index of the composite films was estimated using the following equation<sup>[16]</sup>:

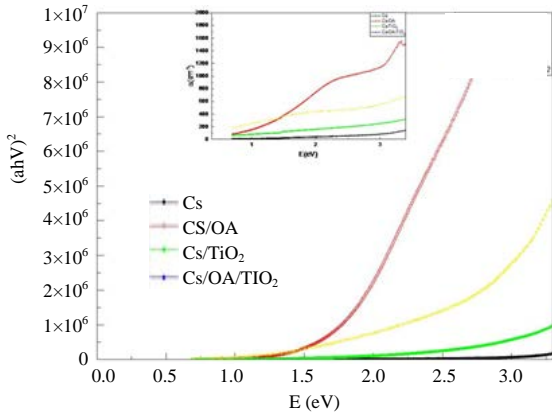


Fig. 4: The relation  $(ahv)^2$  against photon energy,  $hv$  for the films at room temperature

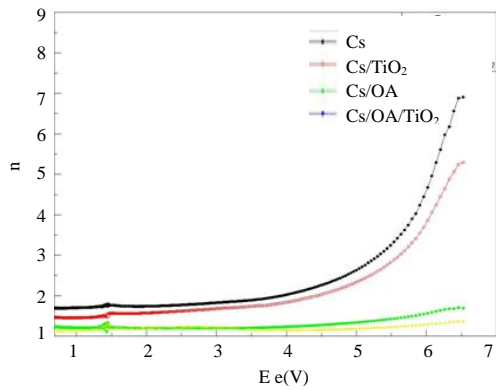


Fig. 5: The variation of refractive index as a function of photon energy for Cs/OA/TiO<sub>2</sub> composite films at room temperature

$$n = \left( \frac{1+R}{1-R} \right) + \sqrt{\frac{4R}{(1-R)^2} - k^2} \quad (4)$$

Figure 5 illustrates the spectral distributions of refractive index of all studied composite films in the energy range 0.6-6.5 eV.

Figure 5 demonstrates that the  $n$  values increase with increasing the photon energy for each sample. In addition, the  $n$  of the composite films decreases with adding TiO<sub>2</sub> and OA.

The lattice dielectric constant,  $\epsilon_L$  and the ratio of number of carrier concentration to electron effective mass  $N/m^*$  can be calculated from the intercept and the slope of the straight-line parts for each Cs/TiO<sub>2</sub> (NPs)/OA composite films according to Eq. 5 from (Fig. 6). All

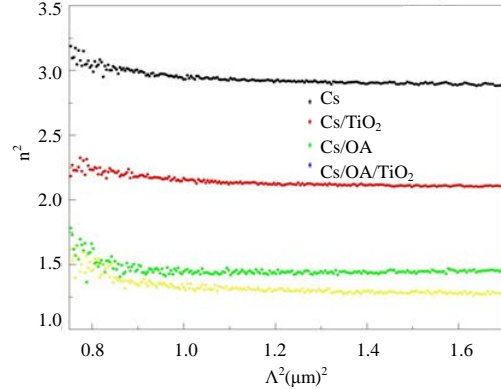


Fig. 6:  $n^2$  versus  $\lambda^2$  for Cs/OA/TiO<sub>2</sub> composite films

Parameters/sample name	$N/m^*$ (number $kg^{-1}$ )	$\epsilon_L$
Cs	$1.186 \times 10^{53}$	2.01
Cs/TiO <sub>2</sub>	$8.70 \times 10^{55}$	1.45
Cs/OA	$3.70 \times 10^{54}$	1.41
Cs/OA/TiO <sub>2</sub>	$3.61 \times 10^{56}$	1.54

extracted parameters are listed in Table 2. The table reveals that the increase with adding TiO<sub>2</sub> and OA while  $\epsilon_L$  decrease:

$$\epsilon_1 = n^2 = \epsilon_L - \left( \frac{e^2 N}{\pi C^2 m^*} \right) \lambda^2 \quad (5)$$

The obtained values of refractive index,  $n$  and absorption index,  $k$  have been used to calculate the real ( $\epsilon_1$ ) and imaginary ( $\epsilon_2$ ) parts of the dielectric constants, (Fig. 7) following the relations (Eq. 6)<sup>[17]</sup>:

$$\epsilon_1 = n^2 - k^2, \epsilon_2 = 2nk \quad (6)$$

Figures 8 illustrate the complex optical conductivity (real  $\sigma_1$  and imaginary,  $\sigma_2$ ), The volume energy loss function, VELF and the surface energy loss function, SELF (Fig. 9). These parameters can be calculated in terms of the real and imaginary parts of the dielectric constant following the relations (Eq. 7 and 8)<sup>[16]</sup>. The value of real conductivity that confirm decreasing in energy gap with increase concentration of TiO<sub>2</sub> nanoparticles:

$$\sigma_1 = \omega \epsilon_0 \epsilon_2, \sigma_2 = \omega \epsilon_0 \epsilon_1 \quad (7)$$

$$VELF = \frac{\epsilon_2}{\epsilon_1^2 + \epsilon_2^2}, SELF = \frac{\epsilon_2}{(\epsilon_1 + 1)h + \epsilon_2^2} \quad (8)$$

The optoelectronic crucial parameters can be obtained such as relaxation time,  $\tau$ , optical mobility,  $\mu_{opt}$ , optical resistivity,  $\rho_{opt}$  and optical electronegativity,

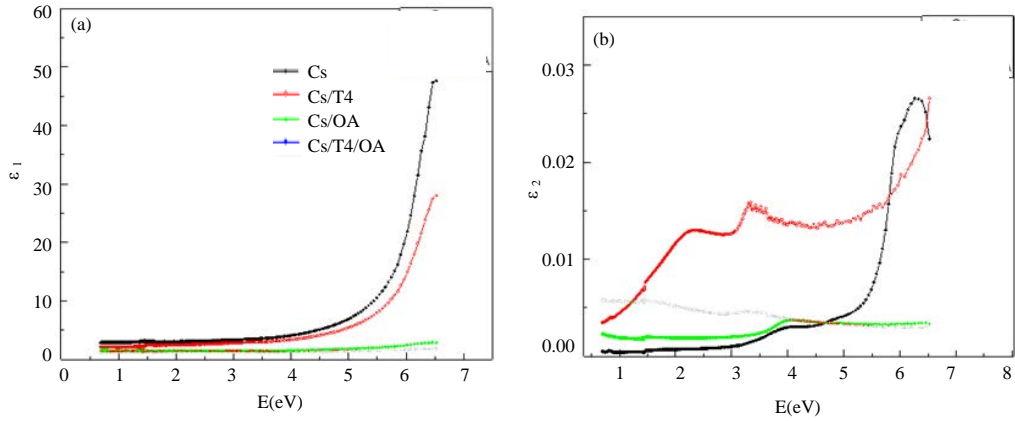


Fig. 7 (a, b): The variation of (a) the real dielectric constant,  $\epsilon_1$  and (b) the imaginary dielectric constant,  $\epsilon_2$  as functions of photon energy for Cs/OA/TiO<sub>2</sub> composite films

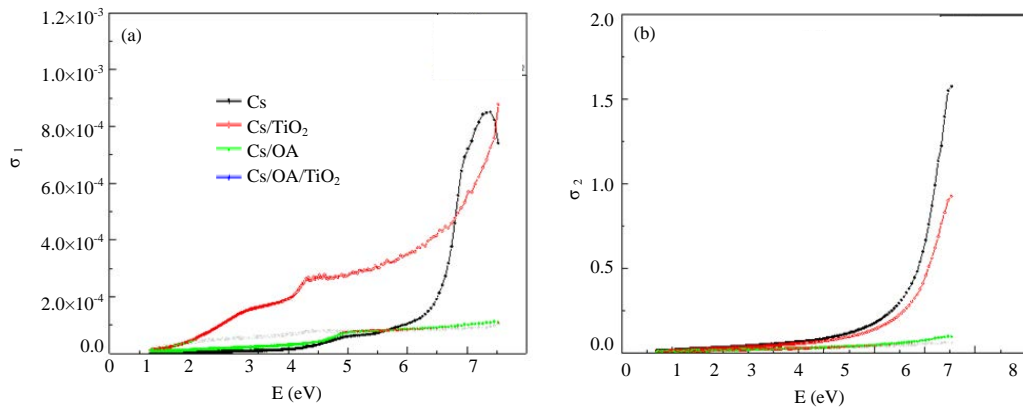


Fig. 8 (a, b): Photon energy dependence of (a) real optical conductivity and (b) imaginary optical conductivity for Cs/OA/TiO<sub>2</sub> composite films

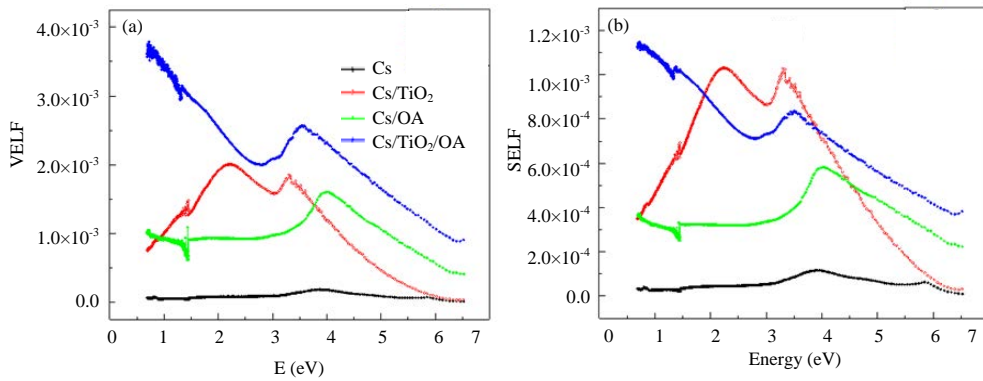


Fig. 9 (a-b): Photon energy dependence of (a) the volume energy loss, VELF and (b) surface energy loss, SELF, factors for Cs/OA/TiO<sub>2</sub> composite

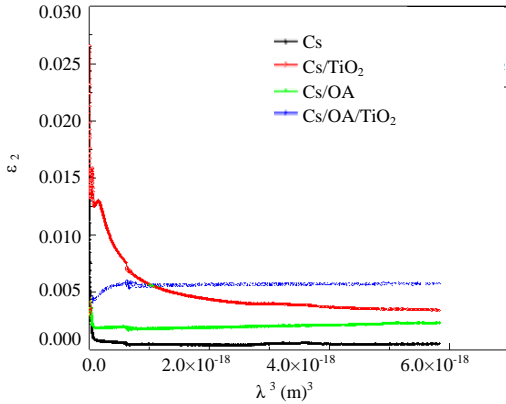


Fig. 10: Variation of the optical imaginary part of dielectric,  $\epsilon_2$ , versus  $\epsilon_3$  for all studied composite films

Table 3: The values of the  $E_g$ ,  $\tau$ ,  $\mu_{opt}$ ,  $\rho_{opt}$  and  $\eta_{opt}$  for Cs/OA/TiO<sub>2</sub> composite films

Samples	$\tau$ (sec)	$\mu_{opt}$	$\rho_{opt}$	$\eta_{opt}$
Cs	$0.70 \times 10^{-13}$	$0.12 \times 10^{-1}$	$0.92 \times 10^2$	1.968
Cs/TiO <sub>2</sub>	$0.91 \times 10^{-13}$	$0.15 \times 10^{-1}$	$0.82 \times 10^2$	2.048
Cs/OA	$2.92 \times 10^{-14}$	$0.52 \times 10^{-2}$	$1.11 \times 10^2$	2.110
Cs/OA/TiO <sub>2</sub>	$1.42 \times 10^{-13}$	$0.246 \times 10^{-1}$	$1.21 \times 10^2$	2.191

$\eta_{opt}$ . The optical relaxation time,  $\tau$  can be estimated for all studied composite films following the equation<sup>[17]</sup>:

$$\epsilon_2 = \frac{1}{4\pi^3 \epsilon_0} \left( \frac{e^2}{c^3} \right) \left( \frac{N_{opt}}{m^*} \right) \left( \frac{1}{\tau} \right) \lambda^3 \quad (9)$$

Figure 10 demonstrates the variation of the imaginary part of dielectric,  $\epsilon_2$ , via. According to this figure, the relaxation time calculated from the slope of the straight line of normal dispersion part. In other words, the measurements of all samples are independent of the scattering mechanism and tabulated in (Table 3).

The optical mobility,  $\mu_{opt} = e\tau/m_0$  and resistivity,  $\rho_{opt} = 1/e \mu_{opt} N_{opt}$ , were calculated for all studied composite films with addition OA and TiO<sub>2</sub>. The optical electro negativity is a crucial parameter for optoelectronic structures of majority compounds and can be calculated using Duffy's Model  $\eta_{opt} = [A/\eta]^{1/4}$  where A is a dimensionless constant and equals 25.54 for majority materials. The estimated values of the nearly constant within experimental error (Table 3), due to the values of the refractive index with different concentration at normal dispersion region. This parameter is the capability of a radical or atom to compose ionic bond by attracting electrons and reveals to many physico-chemical parameters of the materials<sup>[17]</sup>.

### CONCLUSION

In the present work, Chitosan, TiO<sub>2</sub> and oleic acid have been used to synthesis Cs/OA/TiO<sub>2</sub> nanocomposite

films using the conventional casting technique. The measured reflectance spectral has been used to calculate the CIE tristimulus values and generate the chromaticity diagram of all samples. Furthermore, the type of optical transition of Cs/OA/TiO<sub>2</sub> was directly allowed and the values of the optical bandgap,  $E_g$ , decrease with the addition the TiO<sub>2</sub> nanoparticles and oleic acid. Finally, the parameters  $\epsilon_L$  and  $N/m^*$  were estimated for all samples and dielectric constants ( $\epsilon_1, \epsilon_2$ ), complex optical conductivity ( $\sigma_1, \sigma_2$ ) and VELF. Finally, the optoelectronic crucial parameters such as the relaxation time, optical resistivity and mobility as well as the optical electronegativity were estimated for studied composite films.

### REFERENCES

- Emamifar, A., M. Kadivar, M. Shahedi and S. Soleimanian-Zad, 2010. Evaluation of nanocomposite packaging containing Ag and ZnO on shelf life of fresh orange juice. *Innovative Food Sci. Emerging Technol.*, 11: 742-748.
- De Moura, M.R., F.A. Aouada, R.J. Avena-Bustillos, T.H. McHugh, J.M. Krochta and L.H. Mattoso, 2009. Improved barrier and mechanical properties of novel hydroxypropyl methylcellulose edible films with chitosan/tripolyphosphate nanoparticles. *J. Food Eng.*, 92: 448-453.
- Hanafy, M.S., W.M. Desoky, E.M. Hussein, N.H. El Shaer and M. Gomaa *et al.*, 2020. Biological applications study of bionanocomposites based on chitosan/TiO<sub>2</sub> nanoparticles polymeric films modified by oleic acid. *J. Biomed. Mater. Res. Part A.*, Vol. 1, 10.1002/jbm.a.37019
- Xia, Y. and R.C. Larock, 2010. Vegetable oil-based polymeric materials: Synthesis, properties and applications. *Green Chem.*, 12: 1893-1909.
- Ronda, J.C., G. Lligadas, M. Galia and V. Cadiz, 2011. Vegetable oils as platform chemicals for polymer synthesis. *Eur. J. Lipid Sci. Technol.*, 113: 46-58.
- De Espinosa, L.M. and M.A. Meier, 2011. Plant oils: The perfect renewable resource for polymer science?!. *Eur. Polym. J.*, 47: 837-852.
- Bourbon, A.I., A.C. Pinheiro, M.A. Cerqueira, C.M. Rocha, M.C. Avides, M.A. Quintas and A.A. Vicente, 2011. Physico-chemical characterization of chitosan-based edible films incorporating bioactive compounds of different molecular weight. *J. Food Eng.*, 106: 111-118.
- Bengtsson, M., P. Gatenholm and K. Oksman, 2005. The effect of crosslinking on the properties of polyethylene/wood flour composites. *Compos. Sci. Technol.*, 65: 1468-1479.

09. Gumiero, M., D. Peressini, A. Pizzariello, A. Sensidoni, L. Iacumin, G. Comi and R. Toniolo, 2013. Effect of TiO<sub>2</sub> photocatalytic activity in a HDPE-based food packaging on the structural and microbiological stability of a short-ripened cheese. *Food Chem.*, 138: 1633-1640.
10. Nakayama, N. and T. Hayashi, 2007. Preparation and characterization of poly (l-lactic acid)/TiO<sub>2</sub> nanoparticle nanocomposite films with high transparency and efficient photodegradability. *Polym. Degrad. Stab.*, 92: 1255-1264.
11. Siemann, U., 2005. Solvent cast technology-a versatile tool for thin film production. *J. Progress Colloid Polym. Sci.*, 130: 1-14.
12. Guirguis, O.W. and M.T. Moselhey, 2011. Thermal and structural studies of poly (vinyl alcohol) and hydroxypropyl cellulose blends. *Natural Sci.*, 4: 57-67.
13. CIE., 1986. Recommendation on colorimetry. CIE Publication No. 15.2, Central Bureau of the CIE, Vienna, Austria.
14. Prasad, K.K., S. Raheem, P. Vijayalekshmi and C.K. Sastri, 1996. Basic aspects and applications of tristimulus colorimetry. *Talanta*, 43: 1187-1206.
15. El-Nahass, M.M. and W.M. Desoky, 2017. Investigating the structural and optical properties of thermally evaporated 1,3,3-trimethylindolino- $\beta$ -naphthopyrylospiran thin films. *Applied Phys. A.*, Vol. 123,
16. Zeyada, H.M., M.M. El-Nahass, I.K. El-Zawawi and E.M. El-Menyawy, 2010. Structural and optical properties of thermally evaporated 2-(2, 3-dihydro-1, 5-dimethyl-3-oxo-2-phenyl-1H-pyrazol-4-ylimino)-2-(4-nitrophenyl) acetonitrile thin films. *J. Phys. Chem. Solids*, 71: 867-873.
17. Desoky, W.M., M.S. Dawood and M.M. El-Nahass, 2019. Structural and opto-electrical characterization of sodium-2,3-dicyano-5,6-dichloro-1,4-benzoquinone (Na-DDQ) as complex thin films. *Optik*, 178: 351-362.